The background-limited infrared-submillimeter spectrograph (BLISS) for SPICA: a design study

C.M. Bradford[a], James Bock[a], Warren Holmes[a], and the BLISS study team

[a]Jet Propulsion Laboratory, California Institute of Technology, Pasadena, CA;

ABSTRACT

We are developing the Background-Limited Infrared-Submillimeter Spectrograph (BLISS) for SPICA to provide a breakthrough capability for far-IR survey spectroscopy. SPICAs large cold aperture allows mid-IR to submm observations which are limited only by the natural backgrounds, and BLISS is designed to operate near this fundamental limit. BLISS-SPICA is 6 orders of magnitude faster than the spectrometers on Herschel and SOFIA in obtaining full-band spectra. It enables spectroscopy of dust-obscured galaxies at all epochs back to the first billion years after the Big Bang (redshift 6), and study of all stages of planet formation in circumstellar disks.

BLISS covers 35–433 microns range in five or six wavelength bands, and couples two 2 sky positions simultaneously. The instrument is cooled to 50 mK for optimal sensitivity with an on-board refrigerators. The detector package is 4224 silicon-nitride micro-mesh leg-isolated bolometers with superconducting transition-edge-sensed (TES) thermistors, read out with a cryogenic time-domain multiplexer. All technical elements of BLISS have heritage in mature scientic instruments, and many have own. We report on our design study in which we are optimizing performance while accommodating SPICAs constraints, including the stringent cryogenic mass budget. In particular, we present our progress in the optical design and waveguide spectrometer prototyping. A companion paper in Conference 7741 (Beyer et al.) discusses in greater detail the progress in the BLISS TES bolometer development.

Keywords: Bolometer, TES, Far-IR Spectroscopy, Grating

1. INTRODUCTION

The far-IR spectral regime is the repository of half the electromagnetic energy released in the history of stars and galaxies, and offers the only opportunity to probe the details of embedded star and planet formation and the processes in dust-obscured galaxies. Yet the far-IR has remained a relatively unexplored frontier because sensitive far-IR measurements require a combination that has yet to be fully realized: a large cryogenic telescope above the atmosphere and sensitive far-IR focal-plane technologies. The multinational SPICA team is now poised to provide provide this capability. The most important attribute of SPICA is its sub-6 K temperature. *To understand this advantage, consider that at $\lambda = 100\mu m$, even a well-designed passively-cooled $T \sim 80\,\mathrm{K}$ telescope such as Herschel is more than 10,000 times brighter than the natural astrophysical background due to solar-system and Galactic dust. Cooling the telescope to below 6 K virtually eliminates its emission relative to this background.* The sensitivity improvement afforded by a cold telescope can be dramatic, as resoundingly demonstrated with Spitzer's successes in the mid- and far-infrared with only an 85-cm aperture. SPICA is conceived in this same philosophy, and JAXA has invested significantly over the past decade to develop and verify closed-cycle 4-K and 2-K cryocoolers to enable a cryogen-free 5-year mission.

Send correspondence to CMB: e-mail: matt.bradford@jpl.nasa.gov, phone: 818 393 7499

BLISS Study Team: authors above plus M. Kenyon, A. Beyer, M. Werner, M. Rud, T. Prouvé, P. Echternach: JPL; K. Irwin, S. Cho: NIST; M. Harwit, G. Stacey, Cornell U.; G. Helou, L. Armus, P. Appleton: Caltech; J.D. Smith: U. Toledo; U. Gorti: NASA Ames; G. Rieke, E. Egami: U. Arizona; D. Lester, U. Texas, J. Glenn: U. Colorado, M. Malkan: UCLA, D. Dale: U. Wyoming.

The research described in this paper was carried out at the Jet Propulsion Laboratory, California Institute of Technology, under a contract with the National Aeronautics and Space Administration. Copyright 2010 California Institute of Technology. Government sponsorship acknowleged.

Space Telescopes and Instrumentation 2010: Optical, Infrared, and Millimeter Wave,
edited by Jacobus M. Oschmann Jr., Mark C. Clampin, Howard A. MacEwen, Proc. of SPIE
Vol. 7731, 77310S · © 2010 SPIE · CCC code: 0277-786X/10/$18 · doi: 10.1117/12.857779

Downloaded From: http://proceedings.spiedigitallibrary.org/ on 10/31/2016 Terms of Use: http://spiedigitallibrary.org/ss/termsofuse.aspx

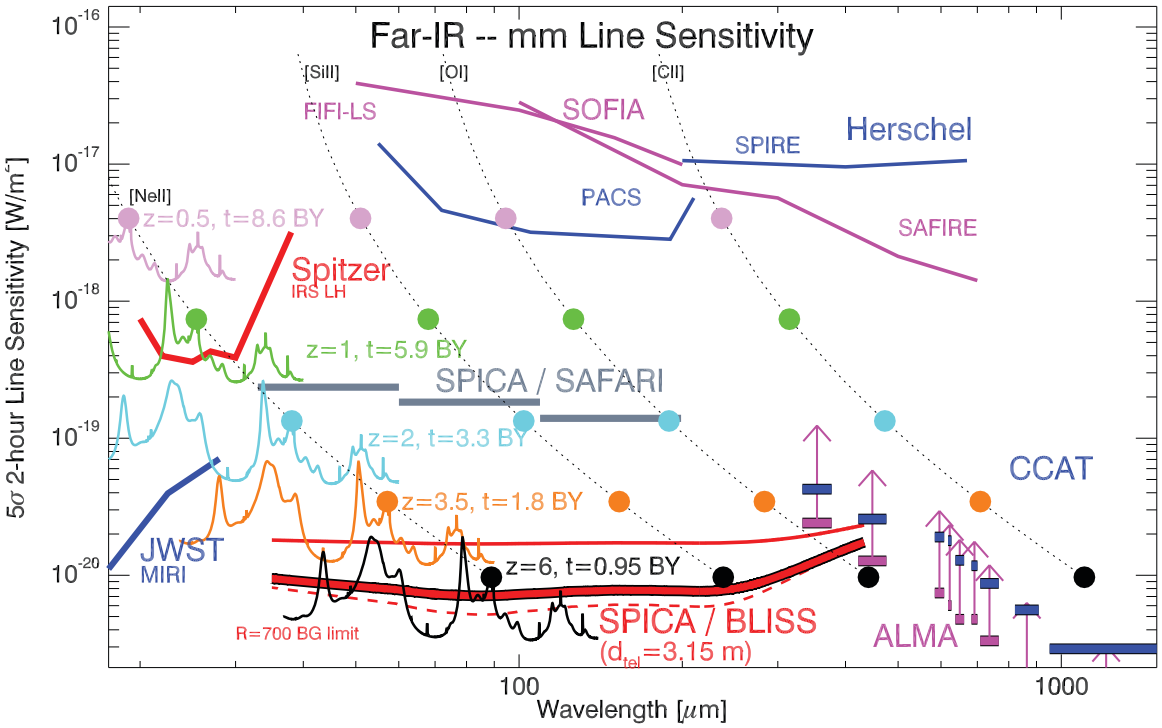

Figure 1. BLISS-SPICA is 100–1000 times more sensitive than present-day far-IR facilities for spectroscopy. (and observing speed scales as the inverse square of the plotted sensitivity.) BLISS sensitivities assume a 3.15-meter SPICA telescope at 5.5 K with 4% emissivity into the beam and 75% aperture efficiency. The spectrometers are assumed to be single-polarization with a transmission of 25%, including the detector quantum efficiency, and the sensitivites refers to an R=700 bandwidth. Chopping the source between the two spectrometers is assumed, and an additional factor of two is included to account for additional losses and inefficiencies. The dashed curved at bottom is the photon background limit, the heavy curve above it assumes the BLISS detector goal sensitivity of $5\times10^{-20}\,\mathrm{W\,Hz^{-1/2}}$. The lighter line above is calculated assuming the BLISS detector sensitivity requirement of $1\times10^{-19}\,\mathrm{W\,Hz^{-1/2}}$. The SAFARI sensitivities are the goal values, taken from the SPICA yellow book, but adjusted to correspond to the 3.15-m aperture. The CCAT curves show sensitivities of proposed spectrographs operating near the background limit on the Cerro-Chaqnantor Atacama Telescope, a 25-meter submillimeter telescope planned for the high Atacama. ALMA sensitivities include arrows which show the penalty associated with multiple tunings to scan an octave of bandwidth. Fine-structure line intensities are shown as dots colored to denote redshift (and age of the Universe), assuming $L_{line}=10^9 L_\odot$. BLISS also has excellent sensitivity to broad features such as the PAH bands—a redshifted $L=10^{12} L_\odot$ galaxy template is plotted, with flux scaled to show the BLISS sensitivity when binned to R=60.

2. SCIENTIFIC PROMISE OF BLISS ON SPICA

The sensitive SPICA platform is especially compelling for wideband spectroscopic follow-up, and BLISS is designed to provide this capability. Over SPICA's 5-year lifetime, BLISS will obtain full-band spectra of thousands of objects ranging from the first dusty galaxies to the most heavily enshrouded young stars and proto- planetary disks in our own Galaxy. These BLISS-SPICA spectra will directly address several pressing scientific concerns, in particular:

2.1 Study the birth of planetary systems.
2.2 Determine the history of cosmic star formation.
2.3 Uncover the connection between galaxies and supermassive black holes.
2.4 Measure the onset of heavy elements and the rise of organic molecules in the Universe.

Downloaded From: http://proceedings.spiedigitallibrary.org/ on 10/31/2016 Terms of Use: http://spiedigitallibrary.org/ss/termsofuse.aspx

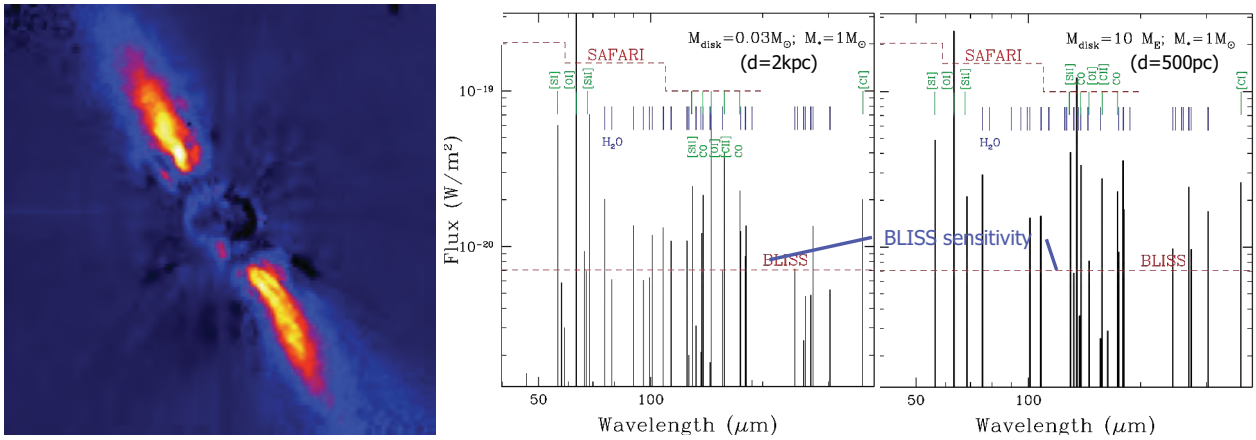

Figure 2. Diagnostics of planet-forming disks accessible with BLISS-SPICA. LEFT: Image of Beta Pic, a nearby (20 pc) disk system. CENTER: Model spectra of a primordial disk with 0.03 $M_\odot$ of gas at 2 kpc. The dust continuum subtracted to show the line fluxes and compare with sensitivities. RIGHT: Model spectrum of an evolved debris disk where only 10 earth masses of gas remains, assuming d = 500pc. BLISS is required for detecting the faint emission lines from these such disks, and enables a comprehensive survey of gas in hundreds of star-forming disks of all ages. (Plotted BLISS and SAFARI sensitivities not yet corrected for the 3.1-m SPICA telescope diameter).

2.1 Planetary-System Formation in the Milky Way: Gas in Disks

The evolution of circumstellar disks and their **gas** component is key to planet formation. Disks rapidly evolve from the primordial gas-rich phase to planetary systems largely devoid of gas, placing stringent time constraints on the availability of gas for giant planet formation according to leading core accretion theories.[1] Even small amounts of residual gas at late stages can affect the settling and radial drift of dust grains, planetary migration and eccentricity evolution.[2–4] Spitzer mid-infrared spectroscopy has detected many atomic, ionic and molecular gas emission lines that arise from the inner 1–20 AU regions of disks, but the bulk of the disk mass is in the outer disk that emits primarily in the far-IR.

BLISS is ideal for studying gas in disks throughout the evolutionary sequence, from very young, primordial massive disks (with ∼0.01 $M_\odot$) to older, evolved disks with tiny amounts (∼ 1 M_{Earth}) of remnant gas (see Figure 2). The various emission lines in the BLISS band originate from different regions of the disk and will trace the surface density distribution of disks as they evolve, form planets and eventually dissipate. *The BLISS sensitivity is crucial for the full evolutionary census.* Herschel/SPIRE is limited to the local (d<150 pc) star-forming environments where only low-mass star formation occurs. The high sensitivity of BLISS will enable us to detect gas emission from circumstellar disks around stars at kiloparsec distances, thus sampling many dense young clusters in giant molecular clouds, the dominant sites for low and high-mass star (and likely planet) formation.

2.2 Charting the Cosmic History of Star Formation

Far-IR and submillimeter continuum imaging surveys are now revealing cosmologically-significant populations of high-redshift galaxies which are so highly obscured that they emit nearly all of their energy in the mid-IR through submillimeter. These datasets, as well deep X-ray surveys show that much of the formative growth of stellar populations and black holes has been deeply obscured by dust for the bulk of the Universe's history. The high dust obscuration makes these galaxies inaccessible to astronomers' traditional diagnostic toolkit: rest-frame UV-optical spectroscopy. With its excellent spectral sensitivity in the 35–433μm band, BLISS brings a powerful new toolkit to bear on these high-redshift galaxy populations: the rest-frame mid- to far-IR, where the dust becomes optically thin, and the dominant interstellar coolants lie (Figs.3,4). Each BLISS spectrum of a distant galaxy will:

- Immediately provide an unambiguous redshift, or look-back time for the galaxy.

Downloaded From: http://proceedings.spiedigitallibrary.org/ on 10/31/2016 Terms of Use: http://spiedigitallibrary.org/ss/termsofuse.aspx

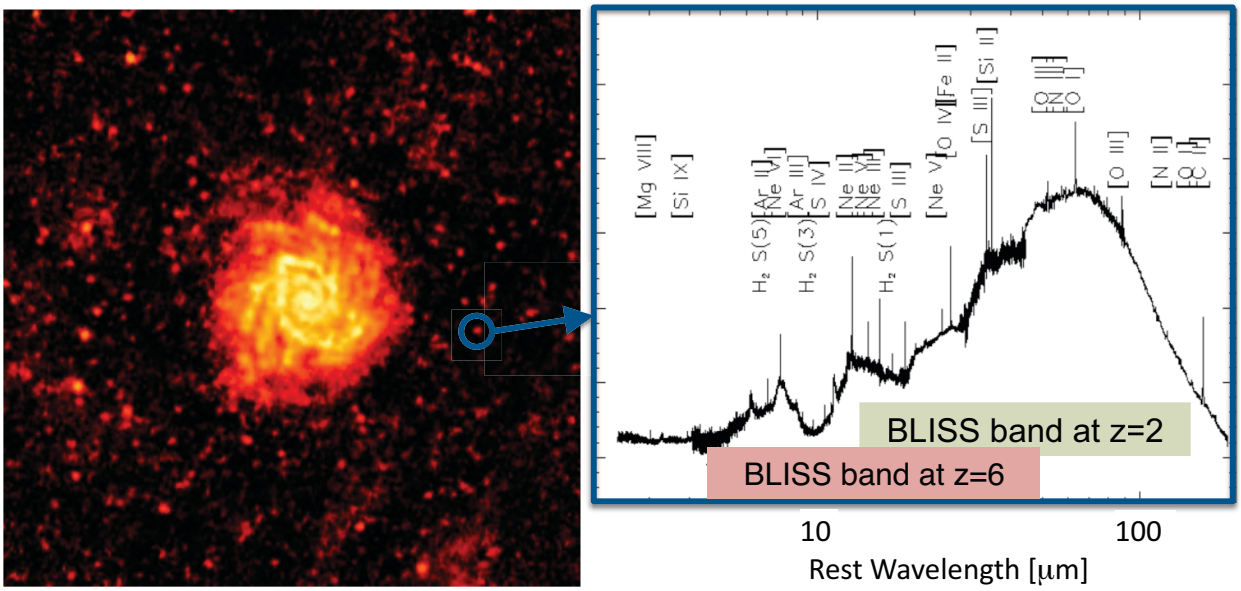

Figure 3. LEFT: Herschel/SPIRE first-light image of M74 observed with the 250μm array, one of the five JPL-built bolometer arrays at the heart of SPIRE. In addition to the central galaxy, numerous far-infrared 'background' galaxies are visible. Most are likely at cosmological redshift (z∼1–5); their light originated in the first half of the Universe's history when star formation was much more vigorous than at present. The spectrometers on Herschel are not sensitive enough for spectroscopy of these galaxies. RIGHT: The Infrared Space Observatory (ISO) spectrum of the Circinus galaxy, a less-luminous nearby analogue of the high-z dusty galaxies. The spectral lines provide a redshift and probe the contents and energy sources deep within the dusty core. SPICA/BLISS will obtain thousands of spectra like this one of galaxies at all ages.

- Determine the total star formation rate in the galaxy and infer a spatial scale of the buried starburst regions by comparing the intensities of the atomic gas coolants—Si^+, C^+, and O^0—with the total far-IR continuum intensity. In aggregate, these measurements chart the time history of dust-obscured stellar power output.
- Measure the stellar initial mass function (IMF) via its effect on the UV field and the resulting ionization structure reflected in the fine-structure lines of ions: O^{++}, Ne^{++}, N^{++}, S^{++}, and N^+, Ne^+. By measuring the IMF verses time, BLISS will confirm or refute the hypothesis of a top-heavy IMF when the Universe was half its age, proposed to explain the discrepancy between stellar mass and energy release measurements.

2.3 Revealing the Black-Hole–Galaxy Connection

Accretion onto black holes (aka active galactic nuclei–AGN) is the second principal energy source in galaxies and it can be substantial. In the local-universe, ultraluminous infrared galaxies (ULIRGs) may derive up to 40% of their power from buried AGN,[5,6] and stacking of faint $1 < z < 3$ ULIRGs selected with Spitzer at 24μm also suggests a significant contribution from buried AGN to the total FIR background power.[7,8] Moreover, there are indications that periods of significant black hole growth are associated with episodes of enhanced host-galaxy star formation, both from models and observations.[9–11] This is intriguing, but spectroscopic confirmation is required to establish the presence of AGN, measure the partitioning of the energy between the AGN and star formation, and study the interaction between the AGN and the host galaxy. The same wideband far-IR spectra that probe the star-formation properties will also find and study buried AGN in the early Universe via:

- Direct measurement of the plasma around the accretion zone itself with fine-structure transitions of high-ionization-state species such as Ne^{4+} and O^{3+} (I.P. 97 & 54 eV).
- Discovery of the warm (∼1000 K), dense (10^7 cm^{-3}) molecular torus believed to exist around the AGN—a likely waypoint as material is funneled from the host galaxy down to the accretion zone. It is expected to emit strongly in the high-J CO rotational transitions (λ_{rest} ∼50–80 μm), easily detectable with BLISS to z=4.

Downloaded From: http://proceedings.spiedigitallibrary.org/ on 10/31/2016 Terms of Use: http://spiedigitallibrary.org/ss/termsofuse.aspx

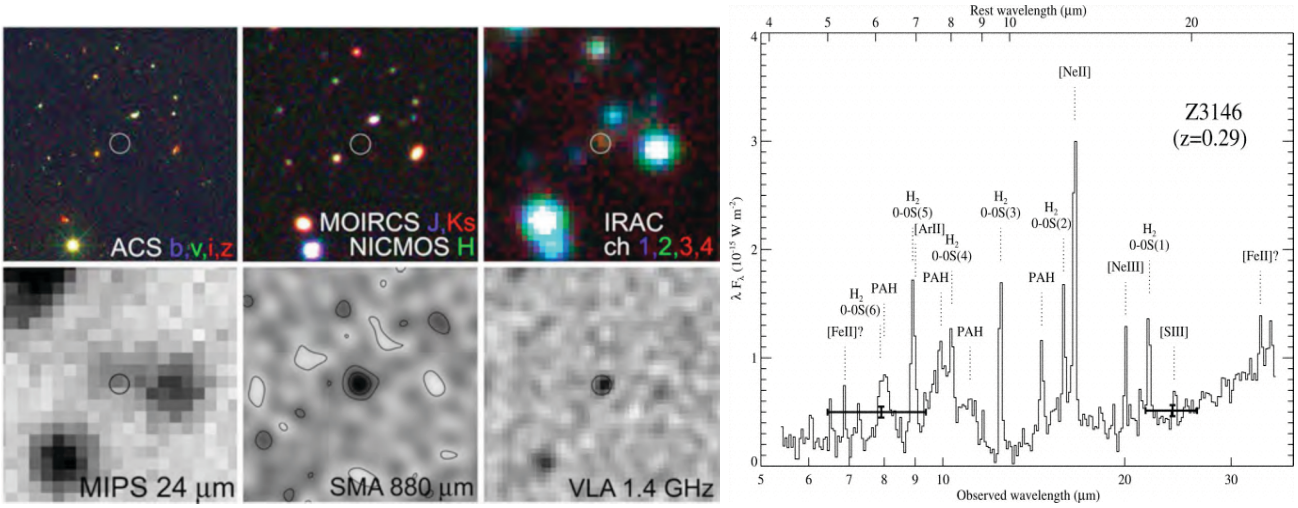

Figure 4. LEFT: Multiwavelength images (24″ on a side) toward a submillimeter-bright galaxy discovered with Scuba/JCMT in the GOODS-N field and confirmed using the SMA submillimeter interferometer (center bottom) which provides an accurate position (from Wang et al. 2009[12]). The object is undetected in deep HST/ACS, HST/NICMOS, and Subaru/MOIRCS images, and is very faint in the Spitzer IRAC, Spitzer MIPS-24 μm, and VLA images. The redshift is unknown but thought to be $z \sim 4-6$. RIGHT: Spitzer IRS spectrum of the Zw 3146 from Egami et al. (2006)[13] showing bright H_2 and PAH emission. These lines and PAH features would be detectable with BLISS - SPICA at z=8–10.

- Study of shocked H_2 generated where AGN outflows impinge upon their host galaxies and the intergalactic medium. Such shocks cool via the H_2 rotational transitions.

2.4 Charting the Rise of Heavy Elements and Organic Molecules

As the Universe is enriched from primordial H_2 to a medium which contains heavy elements and dust grains, the key cooling pathways shift from the quadruple pure rotational H_2 lines (28, 17, 12, 9.7, 8.0, 6.9...μm) to a combination of the fine-structure transitions discussed above and the dust. BLISS will probe all phases of this transition. For metallicity above $\sim 10^{-4}$ solar, fine-structure lines are believed dominate H_2 cooling. However, surprisingly powerful H_2 emitters (e.g., Stephan's Quintet, Zw3146) have been found at low-redshift with Spitzer.[14,15] These nearby sources may be analogs of early-Universe shocks produced in galaxy formation and AGN feedback, when dust and metals are emerging from the first cycles of enrichment. *For z ∼5–10, the H_2 lines are redshifted into the far-IR, and remarkably, Zw3146 itself would be detectable in its H_2 lines with BLISS-SPICA even at z ∼8–10.*

Once heavy elements are in place, the rest-frame mid-IR dust features may actually be the most practical probe of heavy elements at early times. Dust is believed to form as the first heavy elements are created, for example in pair-instability Population III supernovae remnants, and Spitzer has shown that the dust features are often the most powerful features in the spectra of galaxies at all wavelengths. In particular, the polycyclic aromatic hydrocarbon (PAH) features at 6.2–17μm are unambiguous, with to 15× more power than the brightest atomic cooling lines, and act as sensitive probes of heavy element abundance. Like the H_2 lines, they are redshifted out of the JWST band, but not into the ALMA windows in the z ∼5–10 era. BLISS can detect these powerful bands at early epochs (Fig. 1), thus probing the transition from primordial H_2 to heavy-element cooling in the billion years of the Universe.

We emphasize that the excellent sensitivity of BLISS is essential for these distant-galaxy measurements. Charting a complete history requires study of galaxies before, during, and since the putative era of peak star formation and black hole growth between 2–6 billion years after the Big Bang. To reach the first billion of the Universe (z=6) in the spectral probes demands a line sensitivity of $10^{-20}\,\mathrm{W\,m^{-2}}$, which is only achieved with an actively-cooled telescope and a sensitive grating spectrometer such as BLISS.

Downloaded From: http://proceedings.spiedigitallibrary.org/ on 10/31/2016 Terms of Use: http://spiedigitallibrary.org/ss/termsofuse.aspx

Table 1. BLISS Instrument Requirements, Key Technologies, and Heritage

Parameter	Goal	Requirement	Heritage	TRL
Line sens. (5σ, 1h)	1×10^{-20} W m^{-2}	2×10^{-20} W m^{-2}		
Resolving power	700	400		
Spectral coverage	35–433 μm			
Number of beams	2 (source + reference)			
Detector format	4224	2816		
Detector sensitivity	5×10^{-20} W/$\sqrt{\text{Hz}}$	1×10^{-19} W/$\sqrt{\text{Hz}}$		
Detector technology	JPL TES bolometer		BICEP2, SPIDER	4–6
Detector cold readout	NIST time-domain SQUID MUX		BICEP2, SPIDER, ACT, SCUBA2, GISMO	6
Warm electronics	Multi-channel electronics (MCE)		...same...	6
Short-λ spectrometer	Cross-dispersed echelle grating		Spitzer IRS	9
Long-λ spectrometer	WaFIRS waveguide grating		Z-Spec	6
Instrument temperature	50 mK			
Cooler approach	competition sensitive – available upon request		various flight	9

3. BLISS TECHNICAL APPROACH

The scientific objectives require a line sensitivity approaching 10^{-20} W m^{-2}, large instantaneous bandwidth, and moderate spectral resolving power ($R = \delta\lambda/\lambda \geq 400$). The combination of sensitivity and bandwidth is only possible with a grating spectrometer, and the detectors must have sensitivity which is close to the fundamental photon background noise of the zodiacal and Galactic dust. The BLISS wavelength range fills the gap between the 35-μm cutoff of the doped Si BIB arrays (planned for the mid-IR instruments), and the short submillimeter, where observations from the ground with ALMA and single-dish telescopes such as CCAT become practical. These requirements and the key design choices for BLISS are presented in Table 1.

BLISS mounts to the T∼4.5 K SPICA instrument optical bench (IOB). It views an off-axis field through a pickoff mirror located near the edge of the SPICA field to preserve the region near the boresight for the shorter-wavelength instruments. A 3-mirror relay reimages the SPICA focal plane for BLISS; the 2nd relay mirror is at an image of the primary and is chopped to provide beam-switching modulation which is optimal for the bolometers. The relay design has flexibility, and can accommodate a range of positions for BLISS within the IOB, depending on the needs of the other instruments. An example configuration is shown in Figure 5. Thermally, BLISS rejects heat to the SPICA 1.7-K and 4.5-K heat sinks to cool the spectrometers and detectors to 50 mK as well as a thermal intercept stage.

3.1 A Multi-Band Grating Spectrometer

The 38–433μm BLISS range is covered in five or six bands (Table 2), each with its own wideband spectrometer module (Figs. 6,7, 8). We are targeting a resolving power R of 700, but note that for the longest-wavelength

Table 2. BLISS Bands and Bolometer Parameters

Bd.	λ_{min} [μm]	λ_{max} [μm]	Det size [μm] spat	spec	Q [aW]	NEP [10^{-20}W/$\sqrt{\text{Hz}}$] Ph	Det	Mar	G [fW/K]	τ [ms]	Dyn range MoCu	Ti
Cross-Dispersed Echelle Modules												
1	34.5	52.6	TBD		0.12	3.1	2.8	5.0	4	50	400	15000
2	52.6	80.2	TBD		0.12	2.8	2.8	5.0	4	50	400	15000
3	80.2	122	TBD		0.13	2.4	2.8	5.0	4	150	400	15000
Waveguide Far-IR Spectrometer (WaFIRS) Modules												
3	122	186	873	140	0.25	2.6	2.8	5.0	4	150	200	8000
4	186	284	1353	216	0.34	2.4	2.8	5.0	4	150	150	6000
5	284	433	2097	336	2.3	5.0	5.0	5.0	12	150	75	3000

Notes: NEP columns are photon noise, design detector NEP, and detector NEP including margin. Detector noise includes all sources of detector and readout noise with an operating impedance of 10 mOhms with 2 pA/$\sqrt{\text{Hz}}$ unmultiplexed SQUID noise with TES transitions at 65 mK (MoCu) and 450 mK (Ti). Speed of response based on $\alpha = d\ln R/d\ln T = 100$ and a measured heat capacity of 10 fJ/K.

Downloaded From: http://proceedings.spiedigitallibrary.org/ on 10/31/2016 Terms of Use: http://spiedigitallibrary.org/ss/termsofuse.aspx

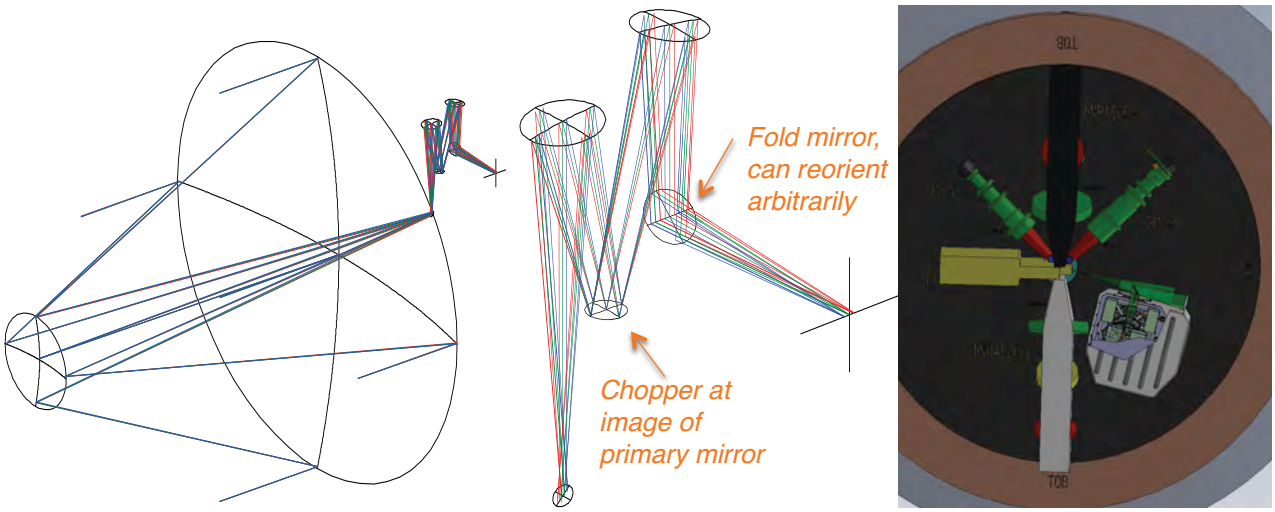

Figure 5. Potential configuration of BLISS on SPICA. LEFT: Optical design of the telescope and the BLISS relay. The BLISS pickoff can be anywhere within the SPICA FOV, here it is shown near the edge at 0.2 degrees from the boresight. The pickoff field of view is set by the two beams and the chopper throw: ∼4–5 arcminutes. CENTER: Relay optics concept: an Offner relay with spherical mirrors, the second mirror is the chopper, at an image of the primary. The final fold mirror is arbitrary. RIGHT: Example position of BLISS within the SPICA IOB. The relay offers flexibility in this positioning to accommodate the needs of the other instruments.

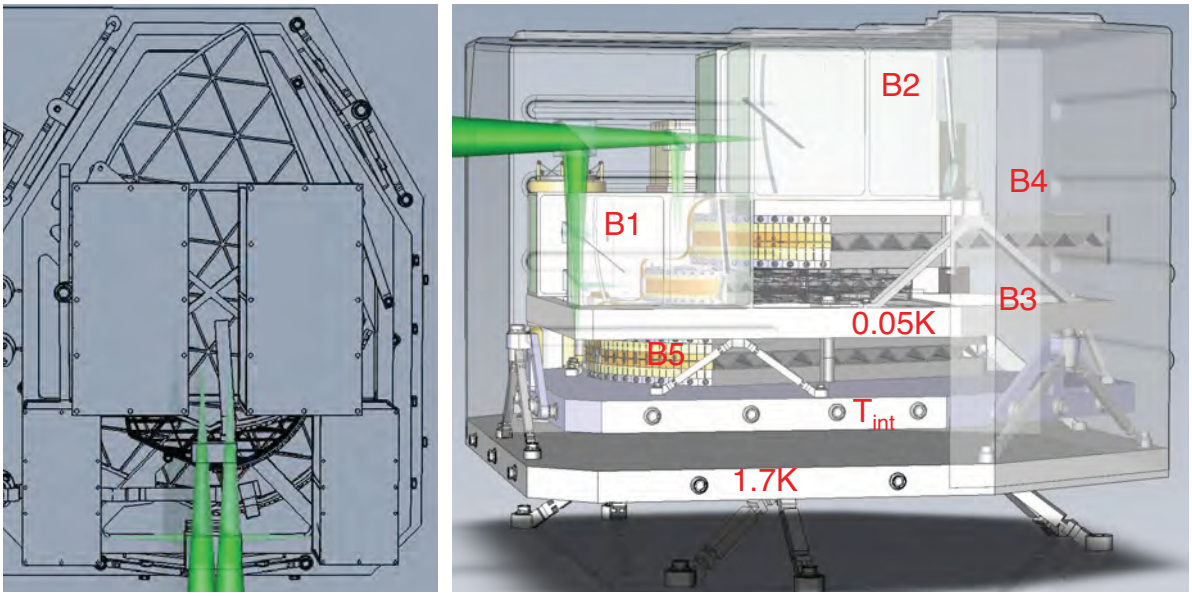

Figure 6. BLISS conceptual layout. This figure showing a 5-band configuration with two echelle modules for each of Bands 1, 2 (four total). The design is evolving toward replacing these four echelle modules with three dual-field modules in three new bands, per Table 2.

band the resolution may have to be reduced since it drives the volume and mass. In the current configuration shown in Figure 6, the longest-wavelength band is limited to R=400, though we are working to increase it. The goal is that all bands will couple the same positions on the sky through the use of a polarizer and dichroic filters. After a polarizing splitter, one linear polarization will couple bands 1, 3, 5 and the other will couple bands 2, 4, 6, easing the requirement on the transition region for the dichroic filters. In this scenario, each spectrometer is only single-polarization, which is a natural property of the long-wavelength spectrometers anyway. The spectrometer bands will each couple two sky positions simultaneously, separated by 2–3 arcminutes (4–6 beams at the longest

Downloaded From: http://proceedings.spiedigitallibrary.org/ on 10/31/2016 Terms of Use: http://spiedigitallibrary.org/ss/termsofuse.aspx

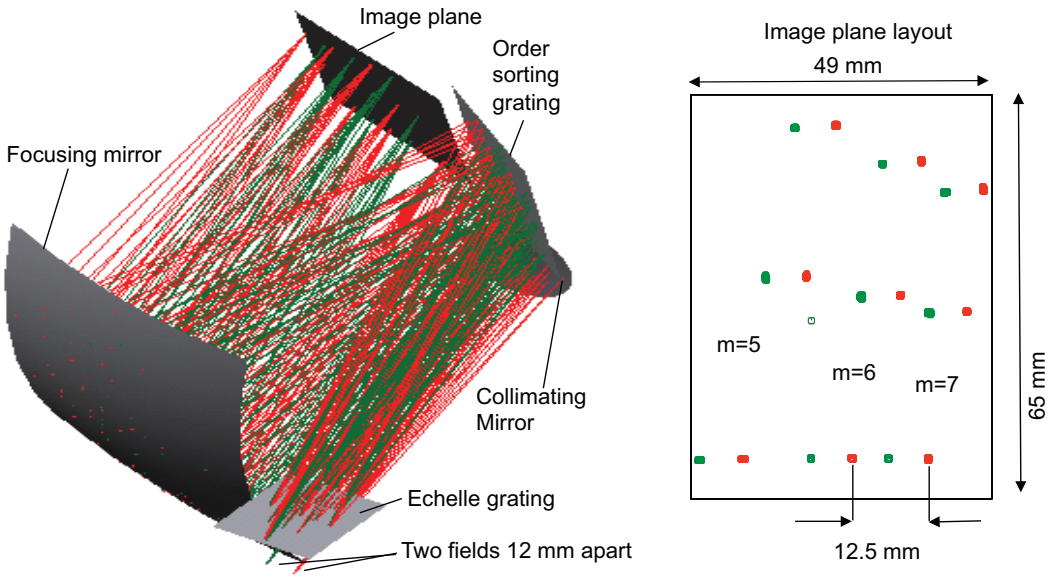

Figure 7. Example design for the dual-beam cross-dispersed spectrograph. This design covers 75 to 120 μm in orders 5, 6, 7, with dimensions of 109×166×155 mm. The spot sizes in the image plane layout indicate the true spot sizes, and the optical performance is diffraction limited. The spacing between the two fields is designed to be half of the minimum order spacing. The bolometers will be arrayed close-packed vertically (the spectral direction), and the layout provides sufficient space for detector legs and wiring between the vertical segments. Not shown is the set of four small flat mirrors near the input (two for each field) which may be required to place the two BLISS fields (separated by 2.5–3 arcmin, ∼20 cm) at a closer spacing of a few $f\lambda$ as required by the order separation in the echelle.

wavelength). The light from the astronomical source will be exchanged between these two spectrometer output positions with the chopping mirror operating at a single fixed frequency between 0.5 and 5 Hz. The dual-field capability provides an important redundancy against loss of a spectral channel in the event of a single detector failing in one field. This is critical for BLISS since without moving parts inside the instrument there is no way to modulate the spectral response with respect to the array, and the spectral sampling is likely to be sub-Nyquist. The dual-field capability also doubles the observing speed.

BLISS will employ two types of broadband grating At the long-wavelengths, conventional free-space grating designs would be too large and massive. BLISS will use the WaFIRS spectrometer architecture: a curved custom-ruled grating in parallel-plate waveguide coupled with a single-mode feed,[19] which offers compact size and small mass. For the short-wavelength BLISS bands, waveguide devices are not an option as they require sub-wavelength manufacturing tolerances, here BLISS will employ conventional cross-dispersed echelle grating modules, similar to those used for the high-resolution modules of the Spitzer infrared spectrograph (IRS),[18] but with a new maximally-compact design. We describe our progress in design and prototyping of both types of spectrometer modules.

3.1.1 Cross-Dispersed Echelle Grating Design

We are studying the design of the echelle grating modules and have developed a 'dual-field' approach, in which a common set of optics couples the light from both separate BLISS fields, and provides sufficient separation in the focal plane to accommodate the quasi-1D bolometer arrays. This enables the dual-field BLISS without the second set of echelle spectrometers, easing the pressure on the mass budget. Figure 7 illustrates the concept. We have found that this approach favors a slightly smaller fractional bandwidth than previously considered for the cross-dispersed echelle, and now baseline that the 35–120 μm range will be covered with three bands each with one of these dual-field modules instead of two bands with two modules each. We anticipate that the reduced bandwidth per module will also improve the blaze efficiency.

Downloaded From: http://proceedings.spiedigitallibrary.org/ on 10/31/2016 Terms of Use: http://spiedigitallibrary.org/ss/termsofuse.aspx

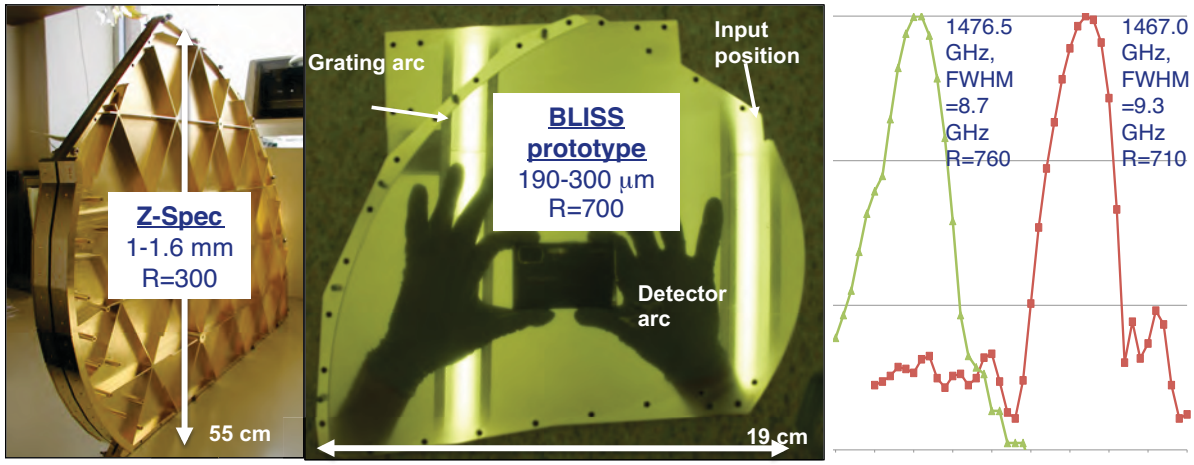

Figure 8. BLISS waveguide spectrometer demonstration. LEFT is the spectrometer with 481 grating facets used in the Z-Spec instrument. It provides R=300 across the 1 mm atmospheric window (0.95–1.65 mm). Center is the BLISS prototype device with a 981-facet grating for 182–303 μm fabricated in the JPL shop (the top plate is removed). Right shows measured spectral profiles of this grating at two nearby frequencies using a local oscillator source and a scanned output feed coupling a 4 K bolometer. The horizontal axis is position of the on the output arc (total range of 2 mm in the plot), and the vertical axis is logarithmic with horizontal lines indicating orders of magnitude. The mapping of frequency to output position, and the resolving power ($\nu/\delta\nu_{\rm FWHM}$) of the system are as designed.

3.1.2 WaFIRS Spectrometer Development

The WaFIRS architecture has been demonstrated on the Z-Spec instrument on Mauna Kea,[16,17] but relative to the Z-Spec module (1-1.6 mm band at R=250–350) both higher frequencies and higher resolving powers are required for BLISS. It is essential to demonstrate this basic capability of the WaFIRS architecture. We have built and begun testing a prototype for the 990 to 1650 GHz band (182–303 μm) with 981 facets in order to provide $R \sim 700$. Our initial measurements show that this device indeed provides the design resolving power, as shown in Figure 8. The WaFIRS spectrometers are an important term in the mass budget, and we also note that our BLISS mass estimates (Table 3) have incorporated sufficient mechanical design and analysis to insure that structures can be built within the mass budget which can survive launch loads for all the bands.

3.2 Transition-Edge-Sensor (TES) Bolometers

BLISS is receptive to any far-IR detector technology which can meet the sensitivity and format requirements on SPICA's timescale. At present, the most viable approach is superconducting TES (transition-edge sensed) bolometer arrays with a SQUID (Superconducting QUantum Interference Device) time-domain multiplexing readout (MUX). The detector is a silicon nitride micro-mesh ('spider-web') bolometer patterned into a metalized grid absorber suspended by thin support legs, with a voltage-biased TES film to sense the thermal power from absorbed radiation. BLISS bolometer parameters are summarized in Table 2. We design the devices to match the total detector noise, dominated by phonon noise $\mathrm{NEP_{phonon}} \simeq \sqrt{4\mathrm{kT^2G}}$, to the photon noise. This determines the thermal conductivity G for a 50 mK base temperature. While detector noise is a significant contribution to the total noise, our criterion is chosen to provide margin on dynamic range to saturation optical power, and sufficient speed of response for our slow-chopped observations. The instrument sensitivities are based on a target detector $\mathrm{NEP} = 5 \times 10^{-20}\,\mathrm{W\,Hz^{-1/2}}$, but we are actually targeting a somewhat lower $3 \times 10^{-20}\,\mathrm{W\,Hz^{-1/2}}$ for the phonon noise itself, thereby providing additional margin for noise sources associated with imperfect instrument interfaces (e.g. EMI/EMC, straylight, etc). To enable both the excellent faint-source sensitivity and adequate dynamic range for Galactic observations, the TES is a dual design using MoCu for low-background observations, in series with elemental Ti for high-background observations. We have demonstrated the design thermal conductance and heat capacity, and have measured NEPs consistent with phonon noise at 220 mK. Measurements of T∼65 mK devices are now underway. *Our BLISS bolometer development progress is summarized in Figure 9, but is presented in greater detail by A. Beyer et al. in SPIE Proceedings Volume 7741.*[20]

Downloaded From: http://proceedings.spiedigitallibrary.org/ on 10/31/2016 Terms of Use: http://spiedigitallibrary.org/ss/termsofuse.aspx

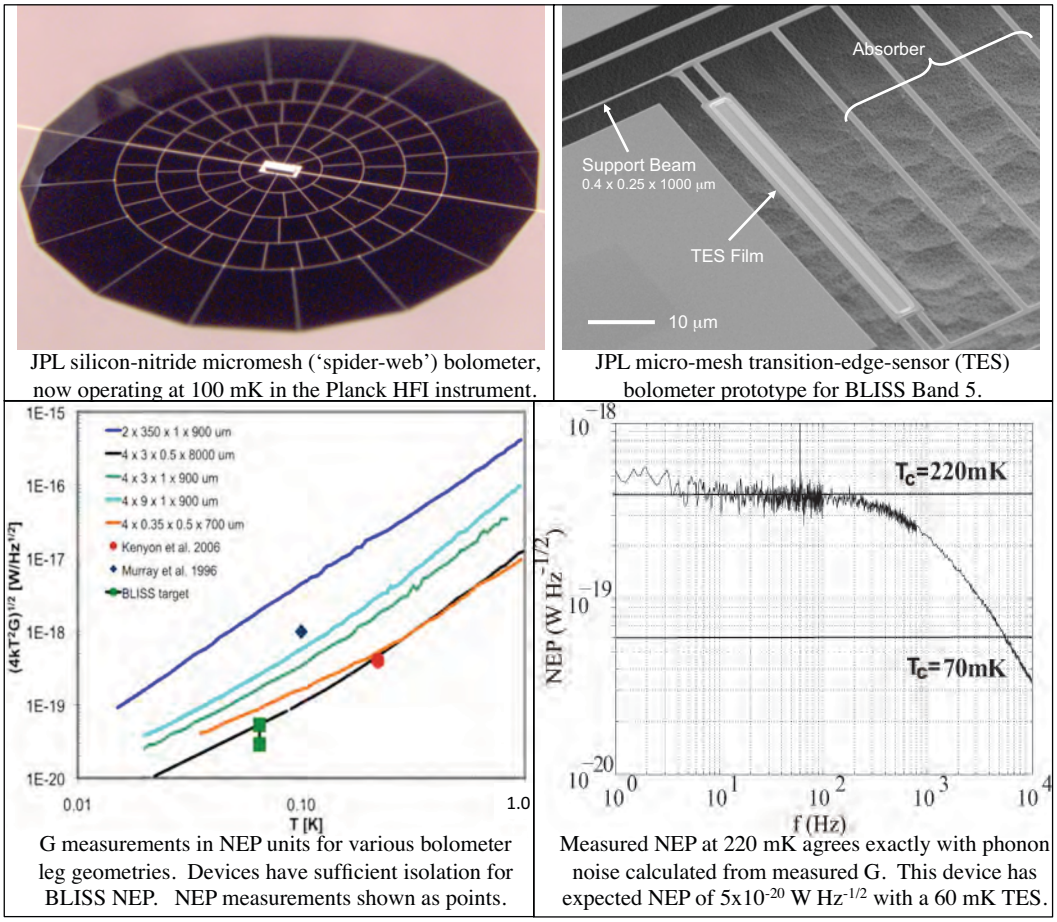

JPL silicon-nitride micromesh ('spider-web') bolometer, now operating at 100 mK in the Planck HFI instrument.

JPL micro-mesh transition-edge-sensor (TES) bolometer prototype for BLISS Band 5.

G measurements in NEP units for various bolometer leg geometries. Devices have sufficient isolation for BLISS NEP. NEP measurements shown as points.

Measured NEP at 220 mK agrees exactly with phonon noise calculated from measured G. This device has expected NEP of 5×10^{-20} W $Hz^{-1/2}$ with a 60 mK TES.

Figure 9. BLISS low-G transition-edge superconducting (TES) bolometer development.

3.3 Cold Multiplexer and Warm Readout Electronics

Cryogenic multiplexing of the bolometer signals enables the moderate format arrays used in BLISS. Technology for cryogenic multiplexing of TES bolometers is rapidly maturing, and SQUID-based time-domain multiplexed (TDM) readouts developed at NIST Boulder are currently able to multiplex up to 40 detectors at the low-temperature stage, introducing negligible amplifier noise. These readouts are being employed in numerous ground-based and sub-orbital experiments. We are collaborating with NIST to develop a MUX suited to the BLISS requirements. The readout will use the now-standard 32-element linear MUX architecture,[21] but with modifications for BLISS. We are developing a chip with 1.5 nW power dissipation at the cold stage, accomplished by reducing the critical current of the SQUID switches and increasing the SQUID input inductance and shunt resistance. The desired SQUID parameters are not extreme, and are similar to those used in some previous SQUID designs. The SQUID inductors will be gradiometer wound to reduce magnetic field sensitivity. The chips will interface to the detectors though a superconducting RF filter to protect the detectors from RF power, and Nyquist inductors tailored to the BLISS detector speed.

The warm readout and control electronics are derived from the proven systems developed for TDM SQUID focal planes and adapted for space. The BLISS readout will operate at a slower frame rate of 2 kHz, appropriate for the relatively slow detector speed, compared with the 15–20 kHz rate used for ground-based systems. Furthermore since the maximum saturation current on the BLISS detectors is much smaller than the periodic current on the input SQUIDs, the feedback control on the SQUIDs can be simplified, reducing the speed requirements on the D/As. These simplifications allow us to square-wave bias the detector, providing noise stability and reducing magnetic field susceptibility in the SQUID readouts.

Downloaded From: http://proceedings.spiedigitallibrary.org/ on 10/31/2016 Terms of Use: http://spiedigitallibrary.org/ss/termsofuse.aspx

Table 3. BLISS Reference Design: Resource Requirements and SPICA Allocations

Resource	BLISS CBE	Allocation
Cryogenic assembly dimensions [cm]	**∼45×40×40**	**250 dia×50**
Cryogenic mass [kg] (no reserve)	**25.1**	**30**
Relay optics, including chopper drive	2.6	
Beamsplitters & filters	1.0	
50 mK assembly: spectrometer optics & detector blocks	8.3	
Intercept housing, shields and supports	1.3	
1.7 K housing, shields and supports	2.4	
Cryogenic MUX: circuit boards, cables, series array SQUIDs	1.5	
Cooler, including straps, switches, shielding	6.9	
Fasteners	1.1	
Wiring Harness Mass [kg] (no reserve)	15	no constraint
Warm mass (electronics & packaging) [kg] (no reserve)	**23**	**28**
Readout electronics and housing	15	
Chopper / cooler drive / housekeeping electronics + housing	8	
Heat lift at 1.7 K—average in operation [mW]	**2.7**	**5**
Heat lift at 4.5 K—average in operation [mW]	**3.1**	**15**
Heat lift at 1.7 K—standby [mW]	1.5	
Heat lift at 4.5 K – standby [mW]	0.4	
Instrument power in operation [W] (no reserve)	**91**	**<200**
Power system & housekeeping	20	
Sub-K cooler drive & chopper drive	11	
Readout electronics	60	
Instrument power in standby mode [W] (no reserve)	**16**	**<200**
Maximum data rate [Mbits / sec]	**1–2**	**4**

3.4 BLISS Thermal Architecture, Resource Requirements, and Mass Estimate

We have developed a complete thermal model of the BLISS including masses based on optical designs, and a support structure sufficient to survive launch loads. The focal-plane modules are cooled to 50 mK with a system that rejects heat to SPICA's 1.7 K and 4.5 K cooling stages, and the operation of this cooler is modeled including all conducted loads through structures and wiring, radiative loads, as well as the multiplexer dissipation. Appropriate magnetic shielding is included in our mass budget, as is the copper strapping required to insure that thermal gradients are less than 0.5 mK on the cold stage. Table 3 summarizes the BLISS resource requirements and the fiducial SPICA allocations for a US instrument, showing that BLISS fits within the allocations.

ACKNOWLEDGMENTS

We thank Jeremy Hodis and Jonathan Kawamura at JPL for help with the WaFIRS spectrometer measurements.

REFERENCES

1. Hubickyj, O., Bodenheimer, P., and Lissauer, J. J., "Accretion of the gaseous envelope of Jupiter around a 5 10 Earth-mass core," *Icarus* **179**, 415–431 (Dec. 2005).
2. Takeuchi, T. and Lin, D. N. C., "Attenuation of Millimeter Emission from Circumstellar Disks Induced by the Rapid Dust Accretion," *ApJ* **623**, 482–492 (Apr. 2005).
3. Ward, W. R., "Survival of Planetary Systems," *ApJL* **482**, L211+ (June 1997).
4. Kominami, J. and Ida, S., "The Effect of Dissipating Gas Disk on Terrestrial Planet Formation," in [*Bulletin of the American Astronomical Society*], *Bulletin of the American Astronomical Society* **34**, 941–+ (Sept. 2002).
5. Armus, L., Charmandaris, V., Bernard-Salas, J., Spoon, H. W. W., Marshall, J. A., Higdon, S. J. U., Desai, V., Teplitz, H. I., Hao, L., Devost, D., Brandl, B. R., Wu, Y., Sloan, G. C., Soifer, B. T., Houck, J. R., and Herter, T. L., "Observations of Ultraluminous Infrared Galaxies with the Infrared Spectrograph on the Spitzer Space Telescope. II. The IRAS Bright Galaxy Sample," *ApJ* **656**, 148–167 (Feb. 2007).

Downloaded From: http://proceedings.spiedigitallibrary.org/ on 10/31/2016 Terms of Use: http://spiedigitallibrary.org/ss/termsofuse.aspx

6. Farrah, D., Bernard-Salas, J., Spoon, H. W. W., Soifer, B. T., Armus, L., Brandl, B., Charmandaris, V., Desai, V., Higdon, S., Devost, D., and Houck, J., "High-Resolution Mid-Infrared Spectroscopy of Ultraluminous Infrared Galaxies," *ApJ* **667**, 149–169 (Sept. 2007).
7. Papovich, C., Rudnick, G., Le Floc'h, E., van Dokkum, P. G., Rieke, G. H., Taylor, E. N., Armus, L., Gawiser, E., Huang, J., Marcillac, D., and Franx, M., "Spitzer Mid- to Far-Infrared Flux Densities of Distant Galaxies," *ApJ* **668**, 45–61 (Oct. 2007).
8. Daddi, E., Alexander, D. M., Dickinson, M., Gilli, R., Renzini, A., Elbaz, D., Cimatti, A., Chary, R., Frayer, D., Bauer, F. E., Brandt, W. N., Giavalisco, M., Grogin, N. A., Huynh, M., Kurk, J., Mignoli, M., Morrison, G., Pope, A., and Ravindranath, S., "Multiwavelength Study of Massive Galaxies at z˜2. II. Widespread Compton-thick Active Galactic Nuclei and the Concurrent Growth of Black Holes and Bulges," *ApJ* **670**, 173–189 (Nov. 2007).
9. Soltan, A., "Masses of quasars," *MNRAS* **200**, 115–122 (July 1982).
10. Yu, Q. and Tremaine, S., "Observational constraints on growth of massive black holes," *MNRAS* **335**, 965–976 (Oct. 2002).
11. Hopkins, P. F., Hernquist, L., Cox, T. J., Robertson, B., and Krause, E., "An Observed Fundamental Plane Relation for Supermassive Black Holes," *ApJ* **669**, 67–73 (Nov. 2007).
12. Wang, W.-H., Barger, A. J., and Cowie, L. L., "Ultradeep Near-Infrared Observations of Goods 850-5," *ApJ* **690**, 319–329 (Jan. 2009).
13. Egami, E., Rieke, G. H., Fadda, D., and Hines, D. C., "A Large Mass of H_2 in the Brightest Cluster Galaxy in Zwicky 3146," *ApJL* **652**, L21–L24 (Nov. 2006).
14. Ogle, P., Antonucci, R., Appleton, P. N., and Whysong, D., "Shocked Molecular Hydrogen in the 3C 326 Radio Galaxy System," *ApJ* **668**, 699–707 (Oct. 2007).
15. Appleton, P. N., Xu, K. C., Reach, W., Dopita, M. A., Gao, Y., Lu, N., Popescu, C. C., Sulentic, J. W., Tuffs, R. J., and Yun, M. S., "Powerful High-Velocity Dispersion Molecular Hydrogen Associated with an Intergalactic Shock Wave in Stephan's Quintet," *ApJL* **639**, L51–L54 (Mar. 2006).
16. Earle, L., Ade, P., Aguirre, J., Aikin, R., Battle, J., Bock, J., Bradford, C. M., Dragovan, M., Duband, L., Glenn, J., Griffin, G., Hristov, V., Maloney, P., Matsuhara, H., Naylor, B., Nguyen, H., Yun, M., and Zmuidzinas, J., "Z-Spec: a broadband direct-detection millimeter-wave spectrometer -instrument status and first results," *SPIE Conference Series* **6275** (July 2006).
17. Bradford, C. M., Aguirre, J. E., Aikin, R., Bock, J. J., Earle, L., Glenn, J., Inami, H., Maloney, P. R., Matsuhara, H., Naylor, B. J., Nguyen, H. T., and Zmuidzinas, J., "The Warm Molecular Gas around the Cloverleaf Quasar," *ApJ* **705**, 112–122 (Nov. 2009).
18. Houck, J. R., Roellig, T. L., van Cleve, J., Forrest, W. J., Herter, T., Lawrence, C. R., Matthews, K., Reitsema, H. J., Soifer, B. T., Watson, D. M., Weedman, D., Huisjen, M., Troeltzsch, J., Barry, D. J., Bernard-Salas, J., Blacken, C. E., Brandl, B. R., Charmandaris, V., Devost, D., Gull, G. E., Hall, P., Henderson, C. P., Higdon, S. J. U., Pirger, B. E., Schoenwald, J., Sloan, G. C., Uchida, K. I., Appleton, P. N., Armus, L., Burgdorf, M. J., Fajardo-Acosta, S. B., Grillmair, C. J., Ingalls, J. G., Morris, P. W., and Teplitz, H. I., "The Infrared Spectrograph (IRS) on the Spitzer Space Telescope," *ApJS* **154**, 18–24 (Sept. 2004).
19. Bradford, C. M., Naylor, B. J., Zmuidzinas, J., Bock, J. J., Gromke, J., Nguyen, H., Dragovan, M., Yun, M., Earle, L., Glenn, J., Matsuhara, H., Ade, P. A. R., and Duband, L., "WaFIRS: A waveguide far-IR spectrometer: Enabling spectroscopy of high-z galaxies in the far-IR and submillimeter," in [*IR Space Telescopes and Instruments*], Mather, J. C., ed., *Proceedings of the SPIE* **4850**, 1137–1148 (Mar. 2003).
20. Beyer, A. D., Kenyon, M., Bradford, C. M., Bock, J. J., and Echternach, P. M., "Characterizing Silicon Nitride absorbers and support beams for far-IR / submillimeter transition-edge sensors," *Proceedings of the SPIE* **7741** (2010).
21. Reintsema, C. D., Beyer, J., Nam, S. W., Deiker, S., Hilton, G. C., Irwin, K., Martinis, J., Ullom, J., Vale, L. R., and MacIntosh, M., "Prototype system for superconducting quantum interference device multiplexing of large-format transition-edge sensor arrays," *Review of Scientific Instruments* **74**(10), 4500–4508 (2003).

Downloaded From: http://proceedings.spiedigitallibrary.org/ on 10/31/2016 Terms of Use: http://spiedigitallibrary.org/ss/termsofuse.aspx